Precompound emission in low-energy heavy-ion interactions from recoil range and spin distributions of heavy residues: A new experimental method

Manoj Kumar Sharma,[1,*] Pushpendra P. Singh,[2] Vijay Raj Sharma,[3] Mohd. Shuaib,[3] Devendra P. Singh,[4] Abhishek Yadav,[5] Unnati,[6] R. Kumar,[5] B. P. Singh,[3,†] and R. Prasad[3]

[1]*Department of Physics, Shri Varsheny (Postgraduate) College, Aligarh, Uttar Pradesh 202 001, India*
[2]*Department of Physics, Indian Institute of Technology, Ropar, Punjab 140001, India*
[3]*Department of Physics, A.M.U., Aligarh 202002, India*
[4]*Department of Physics, University of Petroleum and Energy Studies, Dehradun, India*
[5]*Inter University Accelerator Centre, New Delhi, 110067, India*
[6]*Department of Physics, Delhi University, Delhi, India*

(Received 17 April 2016; revised manuscript received 16 August 2016; published 26 October 2016)

Recent investigations of heavy-ion reactions at low incident energies have indicated the presence of precompound emission component in considerable strength. In most cases the strength of the precompound component is estimated from the difference in forward-backward distributions of emitted light fast particles and also from the analysis of the measured excitation functions. This paper reports a new method of deciphering the relative contributions of compound and precompound components associated with fusion of ^{16}O with ^{159}Tb, ^{169}Tm, and ^{181}Ta targets by measuring the recoil ranges of heavy residues in an absorbing medium along with the online measurement of the spin distributions in reaction residues produced in the fusion ^{16}O beam with ^{159}Tb and ^{169}Tm targets. Analysis of recoil range and spin distributions of the residues shows two distinct linear momentum-transfer components corresponding to precompound and compound nucleus processes. The input angular momentum associated with precompound products is found to be relatively lower than that associated with compound nucleus process. The precompound components obtained from the present analysis are consistent with those obtained from the analysis of excitation functions.

DOI: 10.1103/PhysRevC.94.044617

I. INTRODUCTION

The experimental observation of emission of light fast particles (LFP), particularly in the heavy-ion reactions at relatively low energies below 6 MeV/nucleon [1], has regenerated interest in the precompound nucleus (PCN) emission process, since it is expected to occur at high energies $\approx$10$-$15 MeV/nucleon [2]. Generally, the relative strengths of compound and precompound components in such reactions are estimated from the enhancement in the flux of emitted LFP in the forward direction over the backward direction. Another method often employed is to analyze the measured excitation functions (EFs) for deviations from the statistical predictions and to attribute them to the PCN emission process. The understanding of the PCN and the compound nucleus (CN) emission in light-ion reactions has been well studied during the past few decades but in heavy-ion reactions it needs to be further explored particularly for those associated with the loss of particles in the primary stage in a very short reaction time (10^{-21} s) prior to the establishment of equilibrated CN [3–8]. The emission of such PCN particles reduces the momentum of the product residues. As such, the measurements of the momentum transfer during the interaction may provide a promising tool for the characterization of the reaction mechanism involved.

Although information about the momentum transfer in heavy-ion reactions may be obtained by several methods [2,9,10], in the present measurements this information has been obtained from the study of the recoil range distributions (RRDs) and the spin distributions (SDs) of the reaction residues. Since loss of particles emitted via the PCN process takes away a significant part of angular momentum, the angular momentum associated with the PCN products is relatively lower than that associated with the CN process. Therefore, in PCN reactions, the residues are populated with relatively less high spin states as compared to the spin states of the residues populated via CN process.

II. MEASUREMENTS AND ANALYSIS OF THE DATA

In order to investigate the role of PCN emission in heavy-ion reactions, three self-consistent measurements i.e., the RRDs, the SDs, and the EFs, have been performed. This paper reports on the measurements of the following: (i) the RRDs for the reactions ^{169}Tm(^{16}O, $2n$)^{183}Ir at incident energy 88 MeV; ^{159}Tb(^{16}O, $2n$)^{173}Ta, ^{159}Tb(^{16}O, pn)^{173}Hf; and ^{159}Tb(^{16}O, $3n$)^{172}Ta at 90 MeV; and ^{181}Ta(^{16}O, $2n$)^{195}Tl reaction at 81, 90, and 96 MeV, respectively; (ii) the SDs for reactions ^{169}Tm(^{16}O, $2n$)^{183}Ir and ^{159}Tb(^{16}O, $2n$)^{173}Ta; and (iii) the EFs for the reactions ^{169}Tm(^{16}O, $2n$)^{183}Ir, ^{159}Tb(^{16}O, $2n$)^{173}Ta, ^{159}Tb(^{16}O, pn)^{173}Hf, ^{159}Tb(^{16}O, $3n$)^{172}Ta, and ^{181}Ta(^{16}O, $2n$)^{195}Tl. Though the experimental details of RRDs [11,12], EFs [11,13], and SDs [14] are given in some

*Corresponding author: manojamu76@gmail.com
†bpsinghamu@gmail.com

of our earlier publications [11–14], a brief description on each is given in the following.

A. Recoil range distributions

An experiment has been carried out at the Inter University Accelerator Centre (IUAC), New Delhi, India, to measure the distribution of ranges of recoiling residues produced both by the CN and the PCN emission processes in $^{16}O + ^{159}Tb$, $^{16}O + ^{169}Tm$, and $^{16}O + ^{181}Ta$ systems. In the RRD experiments, the target followed by a stack of nearly 15 thin Al catcher foils of varying thickness ($\approx$16–45 μg/cm^2 prepared by the vacuum evaporation technique) was mounted in the irradiation chamber normal to the beam direction. Depending on the momentum carried away by the product residues, the recoiling residues were trapped at different ranges in the stack of thin Al foils. The duration of irradiation was about 15 h. The thickness of the catcher foils was measured precisely prior to their use, by measuring the energy loss suffered in each catcher foil by 5.485-MeV α particles from ^{241}Am source. The code SRIM was used for determining the thickness from the energy-loss measurements. The activities induced in each thin catcher were followed off line for about two weeks using a precalibrated high-resolution (2 keV for 1.33-MeV γ ray of ^{60}Co) HPGe detector.

In order to obtain the RRDs, the experimental values of cross section (σ) for the reaction products in different catcher foils were measured by the activation method and then these measured cross sections (σ) of the product residues in each catcher were divided by their respective thicknesses to give the resulting yields. The resulting yields plotted against cumulative catcher thicknesses give the experimental RRDs. The experimental RRD for reaction ^{169}Tm(^{16}O,2n)^{183}Ir is shown in Fig. 1. Solid curve in this figure guides the eye to the experimental RRD data. The bumps (peaks) in the experimental RRD arise due to the overlap of the heavy residues produced via two different reaction mechanisms, i.e., the CN and the PCN emissions of particles. As can be seen from this figure, the experimental RRD data for the reaction ^{169}Tm(^{16}O,2n)^{183}Ir has two peaks, one at a relatively lower value ($\approx$225 μg/cm^2) of cumulative catcher thickness and the other at $\approx$330 μg/cm^2. The peak at $\approx$330 μg/cm^2 corresponds to the fraction of residue produced through the CN process and is consistent with the full momentum transfer events in complete fusion reactions. The peak at relatively smaller range $\approx$225 μg/cm^2 may be attributed to the fact that the residues ^{183}Ir are produced via the PCN process when emission of neutrons takes place prior to the establishment of thermodynamical equilibrium. The emission of two neutrons through the PCN process takes a significant part of momentum as compared to the CN process. Thus, it reduces the momentum of the composite system and hence decreases the range of recoiling residues in the stopping medium. The theoretical simulations of the experimental RRD data for reaction ^{169}Tm(^{16}O,2n)^{183}Ir have also been performed using the code SRIM and the fitting program ORIGIN. A Gaussian peak (shown by blue dotted curve in Fig. 1) corresponding to the CN emission is constructed with ORIGIN program using the following expression;

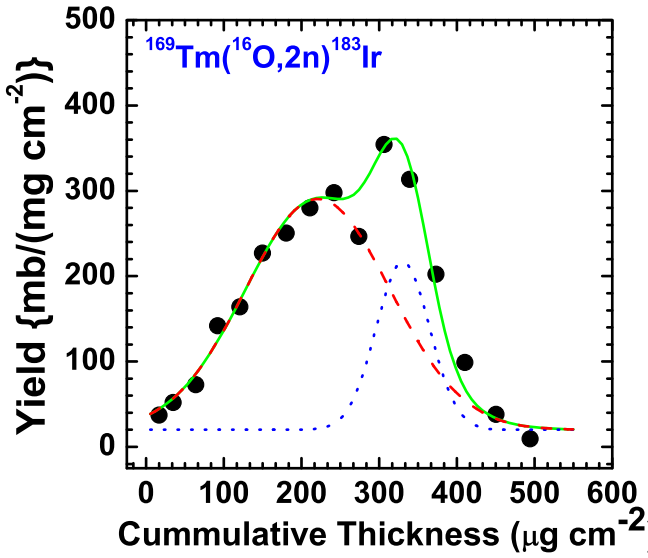

FIG. 1. The experimental RRD for the reaction ^{169}Tm(^{16}O,2n)^{183}Ir at energy $\approx$88 MeV. In this figure a Gaussian peak (blue dotted curve) at higher cumulative thickness represents the CN contribution while the other Gaussian (red dashed curve) at lower thickness represents the PCN contribution. The procedure to decipher the PCN and the CN contributions is discussed in the text.

$$y = y_0 + \frac{A}{w\sqrt{\pi/2}} e^{-2\frac{(x-x_c)^2}{w^2}}, \quad (1)$$

where y_0 = base, x_c = center, A = area under the peak, and w = width (FWHM) are the parameters required for fitting the data for a Gaussian peak of CN emission. The CN Gaussian peak reproduces the experimental data at higher cumulative thicknesses corresponding to the full momentum transfer. In order to find out the contribution of PCN emission, the CN Gaussian peak so constructed by the above procedure has been subtracted from the experimental RRD data. The Gaussian peak (shown by a red dashed curve) at lower cumulative catcher thickness of larger width is obtained, which shows the contribution of PCN emission. By using a similar procedure, the RRDs for reactions ^{159}Tb(^{16}O,2n)^{173}Ta, ^{159}Tb(^{16}O,pn)^{173}Hf, and ^{159}Tb(^{16}O,3n)^{172}Ta have also been measured at $\approx$90 MeV. The experimental RRDs with their theoretical simulations for these reactions are shown in Figs. 2(a)–2(c), respectively. As can be seen from these figures, the experimental RRD data for these reactions have two peaks, one at a relatively lower value of cumulative catcher thickness corresponding to the PCN and the other for the CN at higher cumulative thickness.

In order to judge the reliability (or applicability) of the present method to decipher the CN and the PCN processes and to justify it, the RRDs for the 2n channel in the reaction ^{181}Ta(^{16}O,2n)^{195}Tl at three different energies, 81, 90, and 96 MeV, respectively, have also been measured and are shown in Figs. 2(d)–2(f). The following conclusions may be drawn from Figs. 2(d)–2(f): (i) At each energy, the measured RRD may be resolved in two distinctly different peaks. (ii) Peak corresponding to higher range (full momentum transfer) is

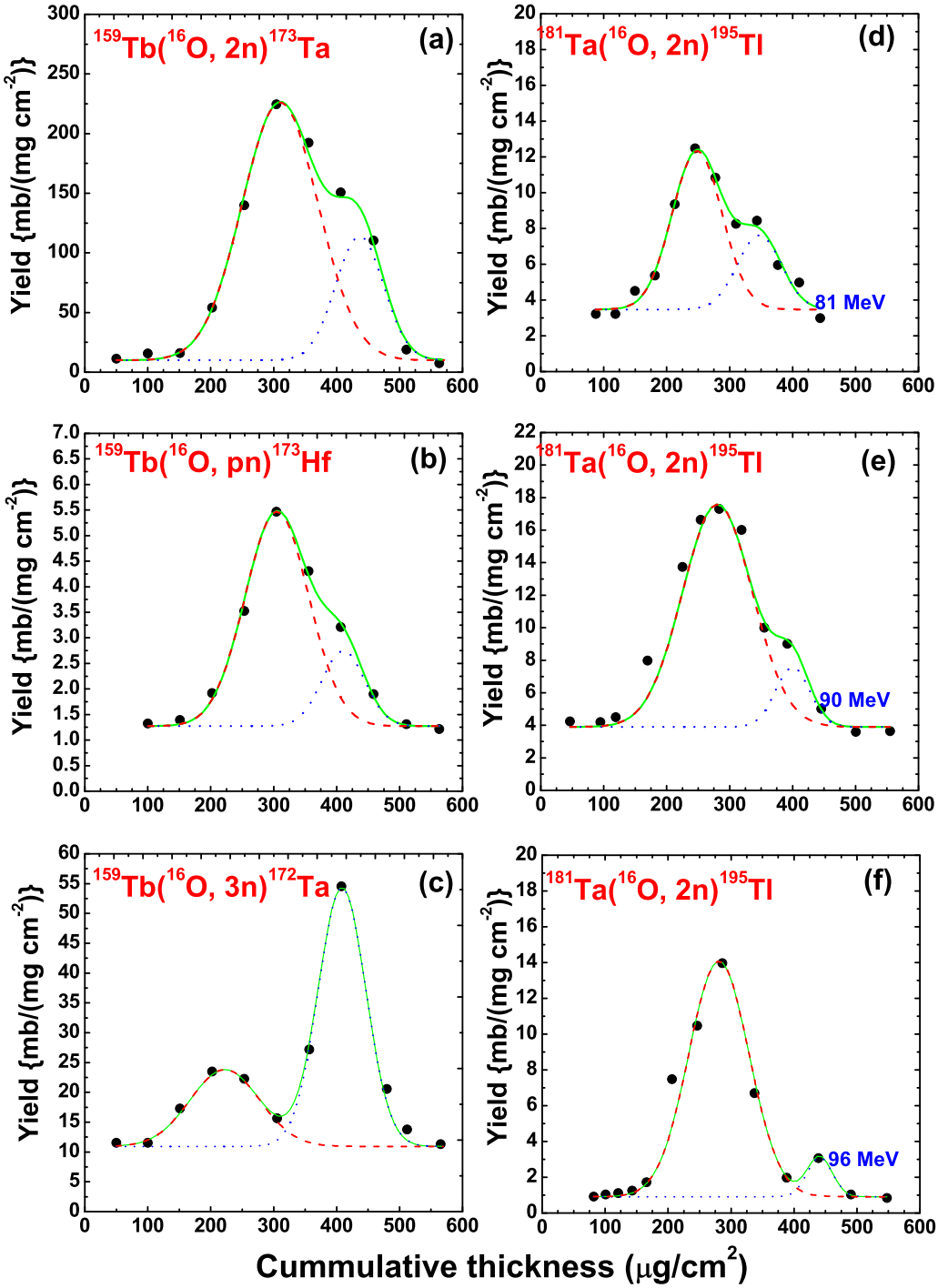

FIG. 2. (a)–(c) The experimental RRDs for the reactions ^{159}Tb(^{16}O,$2n$)^{173}Ta, ^{159}Tb(^{16}O,pn)^{173}Hf, and ^{159}Tb(^{16}O,$3n$)^{172}Ta at energy ≈90 MeV. (d)–(f) The energy-dependent RRD for reaction ^{181}Ta(^{16}O,$2n$)^{197}Tl at energies ≈81, 90, and 96 MeV, respectively.

assigned to the CN process while the peak at lower range is attributed to the PCN process. (iii) As incident energy increases from 81 to 96 MeV, the maxima of both the PCN and the CN peaks shifts towards the higher range side. This is expected since the increase of incident energy increases the linear momentum associated with both the PCN and the CN processes, which in turn results in higher ranges. (iv) It may also be observed from Figs. 2(d)–2(f) that the area under the peak corresponding to the PCN process increases with the increase in incident energy while the area under the CN peak decreases. This reflects that the fact that the relative contribution of the PCN process over that of the CN process increases with incident energy.

In order to deduce the relative contributions of the PCN and the CN processes in these reactions, the areas under the Gaussian peaks corresponding to these processes

have been obtained using the ORIGIN program. The relative contributions of the PCN and the CN processes for the reaction ^{169}Tm(^{16}O,2n)^{183}Ir at 88 MeV are found to be ≈80% and ≈20%, while for reactions ^{159}Tb(^{16}O,2n)^{173}Ta, ^{159}Tb(^{16}O,pn)^{173}Hf, and ^{159}Tb(^{16}O,3n)^{172}Ta at 90 MeV they are ≈70% and ≈30%, ≈73% and ≈27%, and ≈35% and ≈65%, respectively, within the experimental uncertainties (<10%) arising due to various factors, viz., uncertainty in the number of target nuclei due to nonuniformity in sample thickness, the fluctuations in the beam current, uncertainty in the determination of detector efficiency, statistical error in counts, and the dead time of the counting system. The energy-dependent contributions of the PCN and the CN processes in reaction ^{181}Ta(^{16}O,2n)^{195}Tl are found to be ≈68% and ≈32% at 81 MeV, ≈79% and ≈21% at 90 MeV, and ≈88% and ≈12% at 96 MeV respectively. As such, with the increase in energy the PCN contribution is found to increase, as expected.

B. Spin distributions

To further confirm the present findings on the PCN and the CN processes, a second experiment based on particle-γ coincidence technique has been performed at IUAC, New Delhi, India, for measuring the population of spin states during de-excitation of reaction residues. In the present work, the spin distributions of the reaction ^{169}Tm(^{16}O,2n)^{183}Ir at ≈88 MeV and ^{159}Tb(^{16}O,2n)^{173}Ta at ≈93 MeV have been measured using the Gamma Detector Array (GDA) along with the Charged Particle Detector Array (CPDA). The experimental conditions are detailed in Ref. [14]. However, a brief account of the experiment is given here for ready reference.

The GDA is an assembly of 12 Compton suppressed, high-resolution HPGe γ spectrometers arranged at 45°, 99°, and 153° angles with respect to the beam axis and there are four detectors at each of these angles. The CPDA is a set of 14-phoswich detectors housed in a 14-cm-diameter scattering chamber, covering nearly 90% of total solid angle. The reaction residues have been identified from their characteristic prompt γ-transition lines. The proton- and α-emitting channels presented in Ref. [14] have been identified from particle (Z = 1,2)-gated γ spectra. However, neutron-emission channels have been selected from the singles spectra of observed prompt γ transitions collected at forward 45° and backward 153° angles with respect to the direction. The values of relative production yields of the residues (observed area under the peak of the experimentally measured prompt γ lines) have been plotted as a function of observed spin $J_{\rm obs}$ corresponding to prompt γ transitions [15].

In order to have information about the involved input angular momenta and to investigate the entry state spin population of the reaction ^{169}Tm(^{16}O,2n)^{183}Ir, the relative yield has been normalized with minimum observed spin ($J_{\rm obs}^{\rm min}$) at highest yield ($Y_{\rm obs}^{\rm max}$). The experimentally measured SDs obtained from prompt γ rays recorded in forward and backward directions for the reaction ^{169}Tm(^{16}O,2n)^{183}Ir are shown in Figs. 3(a) and 3(b) at 88 MeV, respectively. As can be seen from these figures, the measured SD and hence its decay pattern for this reaction obtained in the forward and backward directions are distinctly different from each other, indicating

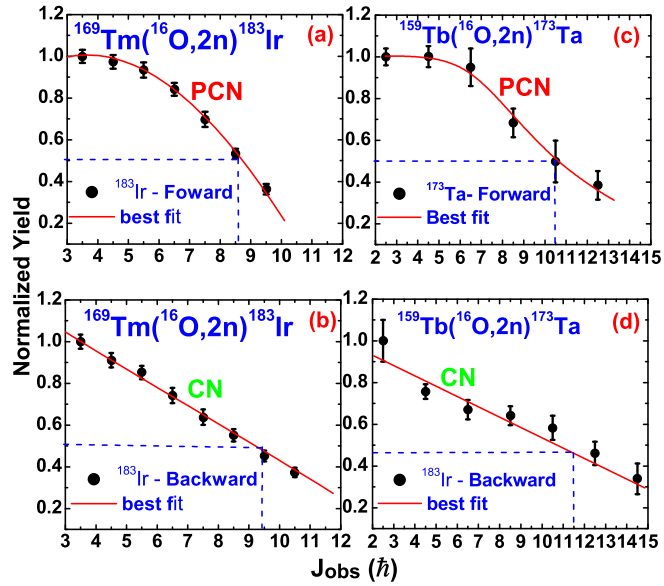

FIG. 3. The experimentally measured spin distributions for reactions ^{169}Tm(^{16}O,2n)^{183}Ir and ^{159}Tb(^{16}O,2n)^{173}Ta in forward and backward directions. The nomenclature used in the plots indicates the involved reaction mechanisms, i.e., the PCN and the CN. The lines and curves through data points are results of best fits.

widely different reaction mechanisms involved. It may be pointed out the entirely different shapes of SDs in forward and backward directions indicate that the two processes are quite different in nature. Further, in the case of CN it is expected that higher spin states in the residues are populated, giving rise to linearly increasing populations of lower spins due to their feeding from the higher spin states. On the other hand, in the case of the PCN, residues are left with relatively lower excitation energy and hence with lower spin entry state; therefore, the feeding of lower spin sates is not linear.

The SDs for the CN and the PCN contributions may be characterized by the parameter, which is termed as the mean input angular momentum associated with the process, specified by the spin where the normalized yield falls to half of its maximum value at lowest observed spin. The mean input angular momenta, i.e., the spin at half yield deduced from experimental SDs of Figs. 3(a) and 3(b) are found to be ≈8.5$\hbar$ and ≈9.5$\hbar$ in forward and backward directions for the reaction ^{169}Tm(^{16}O,2n)^{183}Ir while for reactions ^{159}Tb(^{16}O,2n)^{173}Ta [shown in Figs. 3(c) and 3(d)], it is found to be ≈10.5$\hbar$ and ≈11.5$\hbar$ in forward and backward directions. The observed lower value of the mean input angular momentum in forward direction is due to the fact that emission of LFP (i.e., two PCN neutrons) takes away a significant part of the angular momenta. On the other hand, a relatively higher observed value of the mean input angular momentum in the backward direction is because of the emission of two equilibrated neutrons. As such, it is concluded that distinctly different SDs give direct evidence of the PCN emission process. Thus, the results of the measurements of the SDs further supplement the conclusions drawn from the RRDs measurements. The present work not only strengthens our earlier findings but also provides

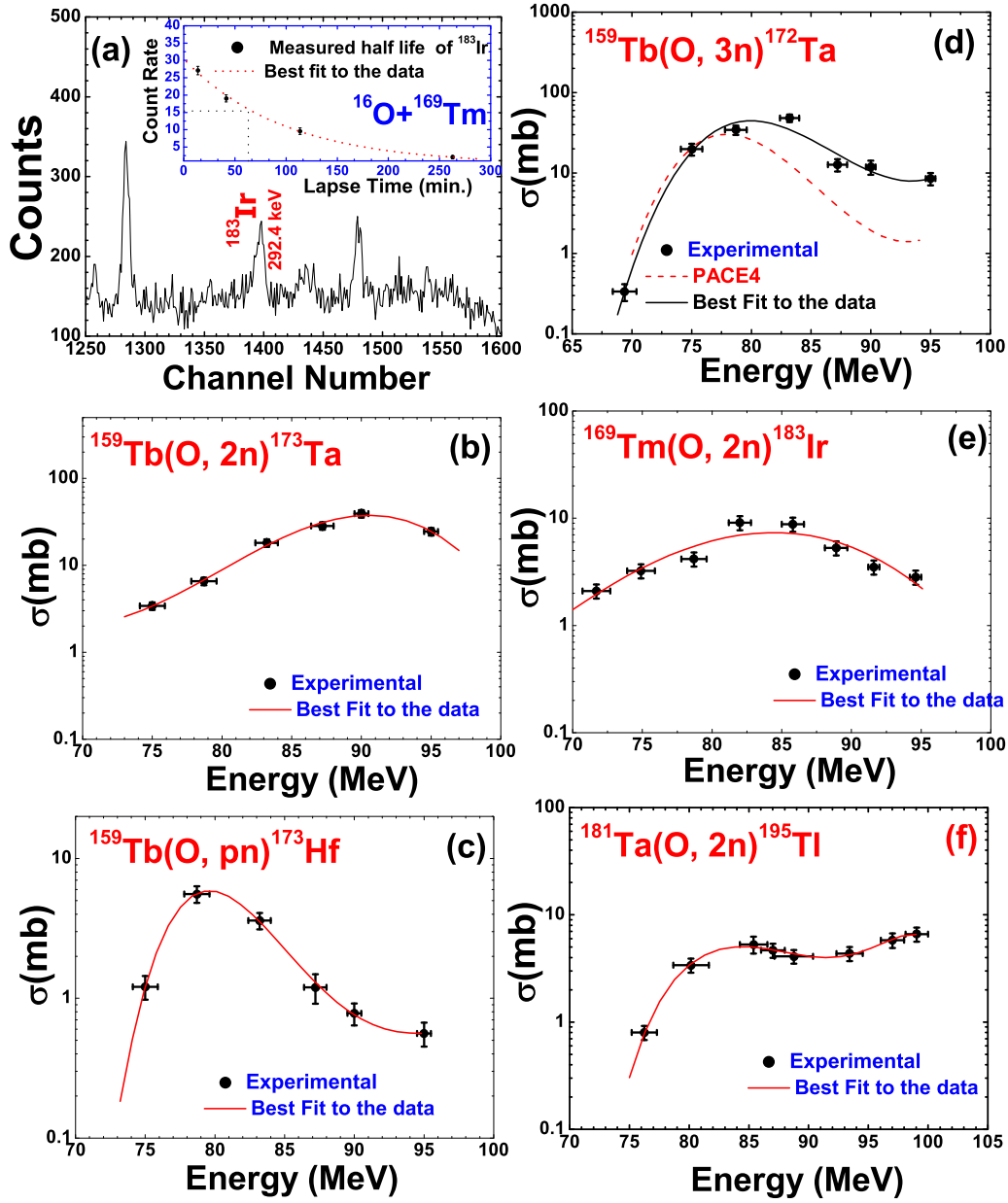

FIG. 4. (a) Observed γ-ray spectrum of ^{169}Tm sample irradiated by ^{16}O beam at ≈88 MeV. The measured decay curve of residues ^{183}Ir is shown in the inset. (b)–(f) The experimentally measured EFs for reactions ^{159}Tb(^{16}O, $2n$)^{173}Ta, ^{159}Tb(^{16}O, pn)^{173}Hf, ^{159}Tb(^{16}O, $3n$)^{172}Ta, ^{169}Tm(^{16}O, $2n$)^{183}Ir, and ^{181}Ta(^{16}O, $2n$)^{195}Tl, respectively. The theoretically calculated EFs by using code PACE4 gives negligibly small values of cross sections for all these reactions except for ^{159}Tb(^{16}O, $3n$)^{172}Ta. For reaction ^{159}Tb(^{16}O, $3n$)^{172}Ta experimentally measured EFs and their PACE4 predictions are also shown in (d).

additional information on the mean input angular momenta associated with the PCN and the CN processes.

C. Excitation functions

As already been mentioned, the deviation of the measured EFs from one calculated theoretical CN mechanism may also be used as a measure of PCN emission. In the present work the EFs for the reactions ^{159}Tb(^{16}O, $2n$)^{173}Ta, ^{159}Tb(^{16}O, pn)^{173}Hf, ^{169}Tm(^{16}O, $2n$)^{183}Ir, ^{159}Tb(^{16}O, $3n$)^{172}Ta, and ^{181}Ta(^{16}O, $2n$)^{195}Tl have been measured in a separate experiments using the stack foil activation technique. In this experiment, the stacks consisting of (^{159}Tb, ^{169}Tm, and ^{181}Ta) target samples followed by Al foils of suitable thickness have been irradiated for ≈8−10 h in a specially designed General Purpose Scattering Chamber (GPSC) 1.5 m in diameter having an in-vacuum transfer facility. The Al foils serve as energy degrader as well as catcher foil where the recoiling residues are trapped. The pertinent decay data required for cross-sectional measurements of the reaction residue have been taken from Ref. [16]. The activities

produced in each target catcher assembly have been measured using a high-resolution large-volume (100 c.c.) high-purity germanium detector (HPGe) γ-ray spectrometer. A typical observed γ-ray spectrum of a ^{169}Tm sample irradiated by an ^{16}O beam at ≈88 MeV is shown in Fig. 4(a). The residues ^{183}Ir have been identified both by its characteristic γ ray and also from the measured half-life. The reaction cross sections for the product residues have been obtained from the measured intensities of the characteristic γ rays using the standard formulation [1].

The analysis of experimental EFs has been performed within the framework of statistical model calculations based on the code PACE4 [17]. The code PACE4 calculates the reaction cross section using the Bass formula [18] through the Monte Carlo procedure. The level density used in this code is calculated from the expression $a = (A/K)$, where A is the mass number of the compound nucleus and K is a free parameter known as the level density parameter constant. In the present work, a value of $K = 8$ is taken in the calculations, which is widely accepted. The detailed discussion of this code along with its parameters are given in Ref. [17].

The experimentally measured EFs for the reactions ^{159}Tb(^{16}O,$2n$)^{173}Ta, ^{159}Tb(^{16}O,pn)^{173}Hf, ^{159}Tb(^{16}O,$3n$)^{172}Ta, ^{169}Tm(^{16}O,$2n$)^{183}Ir, and ^{181}Ta(^{16}O,$2n$)^{195}Tl are shown in Figs. 4(b) to 4(f), respectively. The theoretically calculated EFs using code PACE4 give negligibly small values of cross sections for all these reactions except ^{159}Tb(^{16}O,$3n$)^{172}Ta; hence, these values are not shown in these figures. It means that analysis of EFs gives negligible contribution of CN process for the reaction, while the analysis of RRD for the same reactions gives energy-dependent contributions of the CN and the PCN processes. This shows RRD measurements are much sensitive as compared to EFs. Figure 4(d) shows that the absolute measured cross-sectional values for reaction ^{159}Tb(^{16}O,$3n$)^{172}Ta are higher than predictions of theoretical calculations based on code PACE4 at higher energies. The enhancement of experimentally measured EFs over the theoretical calculations of code PACE4 may be attributed to the PCN emission of a neutron in the first step of de-excitation before equilibration of composite nucleus takes place. Since the PCN emission is not taken into account in the code PACE4, the deviation of the measured data as compared to the theoretical predictions indicate significant contributions of the PCN process over the entire range of energy studied. The analysis of measured EFs for reaction ^{169}Tm(^{16}O,$3n$)^{182}Ir gives a contribution of ≈35% PCN and ≈65% of CN at ≈88 MeV as shown in Fig. 4(d). These data are consistent with the corresponding values obtained from the RRD measurements at ≈88 MeV. Further, the reasonable agreement between the two sets of experiments speaks favorably on the consistency of these measurements.

III. CONCLUSIONS

The experimentally measured recoil rage distributions for the residues produced via the xn channel show a significant contributions due to the PCN process. The results obtained by recoil range distributions are supported by the spin distribution measurements where the mean input momentum involved is found to be lower for the PCN emission than for the CN emission process. The recoil range distribution measurements are found to be a sensitive tool to decipher the CN and the PCN processes. The auxiliary experiments on the excitation function measurements are found to be consistent with both the recoil rage and spin distribution measurements.

ACKNOWLEDGMENTS

The authors are thankful to the director, IUAC, New Delhi, for extending all the facilities for carrying out the experiments. M.K.S. thanks the Council of Scientific and Industrial Research (CSIR), New Delhi, India, Project No. 03(1361)16/EMR-11, for financial support and A. K. Dixit, Principal, S. V. College, Aligarh, for all his support during this work. B.P.S. also thanks DST for providing financial support.

[1] M. K. Sharma, P. P. Singh, D. P. Singh, V. Sharma, A. Yadav, Unnati, I. Bala, R. Kumar, B. P. Singh, and R. Prasad, Phys. Rev. C **91**, 044601 (2015).
[2] J. Gomez del Campo, D. Shapira, J. McConnell, C. J. Gross, D. W. Stracener, H. Madani, E. Cha´vez, and M. E. Ortiz, Phys. Rev. C **60**, 021601(R) (1999).
[3] H. C. Britt and A. R. Quinton, Phys. Rev. **124**, 877 (1961).
[4] T. Otsuka and K. Haradav, Phys. Lett. B **121**, 106 (1983).
[5] P. Vergani, E. Gadioli, E. Vaciago, E. Fabrici, E. Gadioli Erba, M. Galmarini, G. Ciavola, and C. Marchetta, Phys. Rev. C **48**, 1815 (1993).
[6] M. Cavinato, E. Fabrici, E. Gadioli, E. Gadioli Erba, P. Vergani, M. Crippa, G. Colombo, I. Redaelli, and M. Ripamonti, Phys. Rev. C **52**, 2577 (1995).
[7] C. Birattari *et al.*, Phys. Rev. C **54**, 3051 (1996).
[8] H. Delagrance, A. Fleury, F. Hubert, and G. N. Simonoff, Phys. Lett. B **37**, 355 (1971).
[9] H. Morgenstern, W. Bohne, K. Grabisch, D. G. Kover, and H. Lehr, Phys. Lett. B **113**, 463 (1982).
[10] B. B. Back *et al.*, Phys. Rev. Lett. **50**, 818 (1983).
[11] M. K. Sharma *et al.*, Phys. Rev. C **70**, 044606 (2004).
[12] D. P. Singh *et al.*, Phys. Rev. C **81**, 054607 (2010).
[13] P. Descouvemont, T. Druet, L. F. Canto, and M. S. Hussein, Phys. Rev. C **91**, 024606 (2015).
[14] P. P. Singh, B. P. Singh, M. K. Sharma *et al.*, Phys. Lett. B **671**, 20 (2009).
[15] REDWARE level scheme [http://radware.phy.ornl.gov/agsdir1.html].
[16] E. Browne and R. B. Firestone, *Table of Radioactive Isotopes* (Wiley, New York, 1986).
[17] A. Gavron, Phys. Rev. C **21**, 230 (1980).
[18] R. Bass, Nucl. Phys. A **231**, 45 (1974).